Malaysian Journal of Medicine and Health Sciences Vol. 2(2) June 2006: 37-60

Functional Specialisation and Connectivity in Cerebral Motor Cortices : A Single Subject Study Using fMRI and Statistical Parametric Mapping

[1]Ahmad Nazlim Yusoff, [1]Mohd Harith Hashim, [1,2]Mohd Mahadir Ayob, [1]Iskandar Kassim, [1]Nur Hartini Mohd Taib & [3]Wan Ahmad Kamil Wan Abdullah

[1]Diagnostic Imaging and Radiotherapy Programme
Faculty of Allied Health Sciences, Universiti Kebangsaan Malaysia
50300 Jalan Raja Muda Abdul Aziz, Kuala Lumpur
[2]Medical Imaging Programme
Faculty of Health Sciences, Universiti Teknologi MARA, Jalan Osman
Petaling Jaya, Kuala Lumpur
[3]Department of Radiology, School of Medical Sciences
Universiti Sains Malaysia, 16150 Kubang Kerian, Kelantan

ABSTRACT

Objective: A baseline functional magnetic resonance imaging (fMRI) study was carried out on a healthy right-handed male subject to attain further insights into the basic neuronal control mechanisms of bimanual and unimanual movements of hand fingers, an area that is still not fully understood. **Methods :** The study used the basic unimanual and bimanual movements of the left- and right-hand fingers to stimulate neuronal activity in the cerebral cortices. The subject was instructed to sequentially press his fingers either unimanually (UNI) or bimanually (BIM), against the thumb in a consistent alternative manner during the functional scans. The data were analysed using the MATLAB and SPM2 software packages. **Results :** Brain activations obtained via the *F*-test indicate a larger activation area as compared to that obtained from the *T*-test. The results showed that, the activated brain regions due to the self-paced finger movements are the precentral and postcentral gyrii covering the primary motor, premotor and somatosensory primer areas. The active-state signal intensity was found to be significantly ($p < 0.05$) higher than that of the resting-state. For UNI, brain activation showed contra-laterality with a larger activation area and a higher signal intensity at the point of maximum intensity for the left-hand finger movement (UNI_{left}) compared to the right-hand finger movement (UNI_{right}). Small ipsi-lateral activations were observed during UNI_{right} and UNI_{left}. For BIM, the activation was observed in both hemispheres with the right hemisphere showing a higher signal intensity and coverage. The results support the fact that for a right-handed person performing either UNI or BIM type of movement, the activated motor area on the right hemisphere of the brain (movement of the left hand fingers) experience a higher intensity and larger coverage of hemodynamic response compared to the left hemisphere of the brain (movement of the right hand fingers). Analyses performed on the activated regions of interest (ROI) by comparing the unimanual and bimanual types of activations revealed that during BIM, there are voxels in the left hemisphere controlling the movement of the left hand fingers (BIM_{left}) and voxels in the right hemisphere controlling the movement of the right hand fingers (BIM_{right}). The interactions observed in this study resemble the existence of interhemispheric connection between both hemispheres during BIM. **Conclusion :** Although

this is a single subject study, the hemodynamic response and the neuronal control mechanism in the cerebral cortices based on the BOLD mechanism can be studied and evaluated using fMRI and SPM.

Keywords : Functional Magnetic Resonance Imaging (fMRI), Blood Oxygenation Level Dependent (BOLD), Statistical Parametric Mapping (SPM)

INTRODUCTION

Functional magnetic resonance imaging (fMRI) is one of the many advanced applications of magnetic resonance imaging (MRI) in which anatomical brain structures and the corresponding part of the brain that participates in specific biological functions can be precisely located and simultaneously studied. [1] It is well known that the fMRI examination can be conducted noninvasively, in the sense that it neither uses ionising radiation nor radioactive tracers to produce images. It is also known that the fMRI examination does not need exogenous contrast media to be administered into the subjects for image enhancement. Nevertheless, this imaging modality can provide neuroscientists with high resolution brain images together with the activations and in any preferable directions, namely axial, coronal, sagittal and even in oblique slice orientations. The ability of fMRI in detecting small metabolic changes in the brain lies in the state-of-the-art of an imaging technique or pulse sequence invented by Mansfield, the Echo Planar Imaging (EPI) [2, 3] and the discovery of a remarkable endogenous contrast agent, the oxyhemoglobin, by Ogawa *et al*. [4,5,6] The invention of EPI and the discovery of oxyhemoglobin as an endogenous contrast agent, hence Blood Oxygenation Level Dependent (BOLD), since then have shed light on a vast number of studies in functional neuroimaging. Activations in the brain due to various physical (motor [7], auditory [8] and visual [9]), psycological (memory [10], learning and attention [11]) and physiological (in response to drugs [12] or inhaled gasses [13]) stimuli can be clearly observed and studied using fMRI. Consequently, such information has led to compilations of fMRI data sets into databases in many imaging neuroscience centres, making possible the production of maps of human brain functions. All these efforts are likely to benefit the clinicians especially in diagnosing the function or wellness of any particular part of the healthy or deseased brain before performing treatment or surgery.

Recent advances in clinical applications of fMRI appear to have feasible means in allowing neuronal disorder to be effectively diagnosed and investigated. [14, 15, 16] The activation signals measured with fMRI are predicated by indirectly measuring the reduction in the concentration of the paramagnetic deoxyhemoglobin which arises from an increase in blood oxygenation (increase in the concentration of the diamagnetic oxyhemoglobin) during neuronal firings. A complete fMRI study will statistically describe the mechanisms which generate contrast in fMRI and will conclude on the particular brain activity involved in various stimuli.[17] The activation patterns in the working human brain can be mapped with high temporal and spatial resolution. The results are very useful for a number of clinical studies (diagnosis and prognosis) especially in the detection and treatment of various kinds of neurological impairments and pathologies and might be able to contribute to the early detection of stroke and epilepsy.

Initial fMRI studies identified visual, somatosensory, auditory and motor activation areas in the primary cortices. The pronounced effects of finger tapping or motor stimulation on the hemodynamic response in the primary motor cortex and cerebellum have been addressed since the inception of the BOLD imaging technique. Despite carrying out a large volume of studies, a number of studies are still being conducted on finger tapping tasks using sophisticated MRI fascilities, new experimental paradigms and data analyses techniques. The reasons behind the popularity and continuation of finger tapping experiments are fourfold: (i) the finger tapping task can be easily performed by the subject; (ii) motor activations are observable in several large areas in the brain with high intensity and thus can be easily detected and analysed; (iii) the angle of study is rather wide and can be focused on several scopes (for example the different effects of unimanual and bimanual taps, the distinctions between contra-and ipsi-laterality of the right and left hands, the effects of the rate of tapping, the difference between self-paced and externally paced movements); and (iv) the possibility of performing investigation into functional connectivity between motor and other types of stimulus. All the previous studies, though appearing to be experimentally conducted in a different manner, were particularly aimed at searching for the exact mechanisms that govern the change in signal intensity during any particular brain activation or BOLD activation mechanism due to a given finger tapping task. To date, the local mechanisms underlying the BOLD signal change have not been fully understood and need more attention.

In this study, functional MRI studies were conducted on a healthy right-handed male subject. The finger tapping task was chosen for this study in order to gain more information on brain activation mechanism due to motor stimulation. This study focussed, in particular, on functional specialisation and connectivity of the motor activation in the cerebral cortices evoked by both the dominant and subdominant hands. Since this work was based on a single subject where the relevance to subject variations were not known, the results obtained might be very useful for future reference in multiple subject study and could also serve as a baseline for future fMRI research in the country, especially on data acquisition, analysis and interpretation.

MATERIALS AND METHODS

Subject

Functional magnetic resonance imaging (fMRI) scans were performed on a healthy male subject. The subject was paid and was given informed consent and screening forms as required by the Research and Medical Research Ethical Committee of Universiti Kebangsaan Malaysia (UKM). The subject was interviewed on his health condition and handedness prior to the scanning session and was confirmed to be healthy and right-handed. The subject was also told not to move his head during the scan. Changes in signal intensity over time from any one voxel can arise from head motion and this would represent a serious confound particularly in fMRI studies. [17] To ensure minimum head movement, immobilising devices were used together with the head coil.

MRI Scans

A functional magnetic resonance imaging (fMRI) examination was conducted at the Department of Radiology, Universiti Kebangsaan Malaysia Hospital. Functional images were acquired using a 1.5 tesla magnetic resonance imaging (MRI) system (Siemens Magnetom Vision VB33G) equipped with functional imaging option, echo planar imaging (EPI) capabilities and a radiofrequency (RF) head coil used for signal transmission and reception. Gradient Echo-Echo Planar Imaging (GRE-EPI) pulse sequence with the following parameters were applied : repetition time (TR) = 1 ms, echo time (TE) = 66 ms, field of view (FOV) = 210 × 210 mm, flip angle (α) = 90°, matrix size = 128 × 128 and slice thickness = 4 mm. Using the midsagittal scout image (TR = 15 ms, TE = 6 ms, FOV = 300 × 300 mm, α = 30°, matrix size = 128 × 128 and magnetic field gradient = 15 mT/m) produced earlier, 16 axial slice positions (1 mm interslice gap) were oriented in the anterior-posterior commissure (AC-PC) plane. This covered the motor cortex and adjacent motor areas such as premotor cortex and supplementary motor cortex. In addition, high resolution anatomical images of the entire brain were obtained by using a strongly T1-weighted spin echo pulse sequence with the following parameters: TR = 1000 ms, TE = 30 ms, FOV = 210 × 210 mm, α = 90°, matrix size = 128 × 128 and slice thickness = 4 mm.

Experimental Paradigm

The subject was instructed on how to perform the motor activation task and was allowed to practice prior to the scanning. The subject had to press all four fingers against the thumb beginning with the thumb-index finger contact and proceeding to the other fingers in sequence which would then begin anew with contact between thumb and index finger. This study used a self-paced finger movement. The tapping of the fingers would approximately be two times in one second (using an intermediate force between too soft and too hard). A six-cycle active-rest paradigm which was alternately cued between active and rest was used with each cycle consisting of 10 series of measurements during active state and 10 series of measurements during resting state. The tapping of the fingers were done unimanually (UNI_{left} or UNI_{right}) or bimanually (BIM_{right} and BIM_{left}) in alternate fashion as can be seen in *Fig. 1(a).* Each functional measurement produced 16 axial slices in 2s (one image slice in 125 ms). The measurement started with the active state. The imaging time for the whole functional scans was 240s (4 minutes) which produced 120 × 16 = 1920 images in total. High resolution T2* weighted images were obtained using the voxel size of 1.64 mm × 1.64 mm × 4.00 mm.

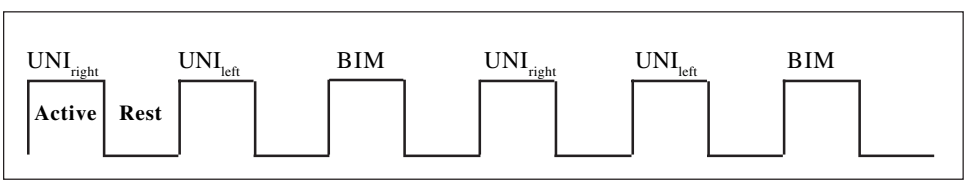

Figure 1(a). The active-rest block paradigm used in this study

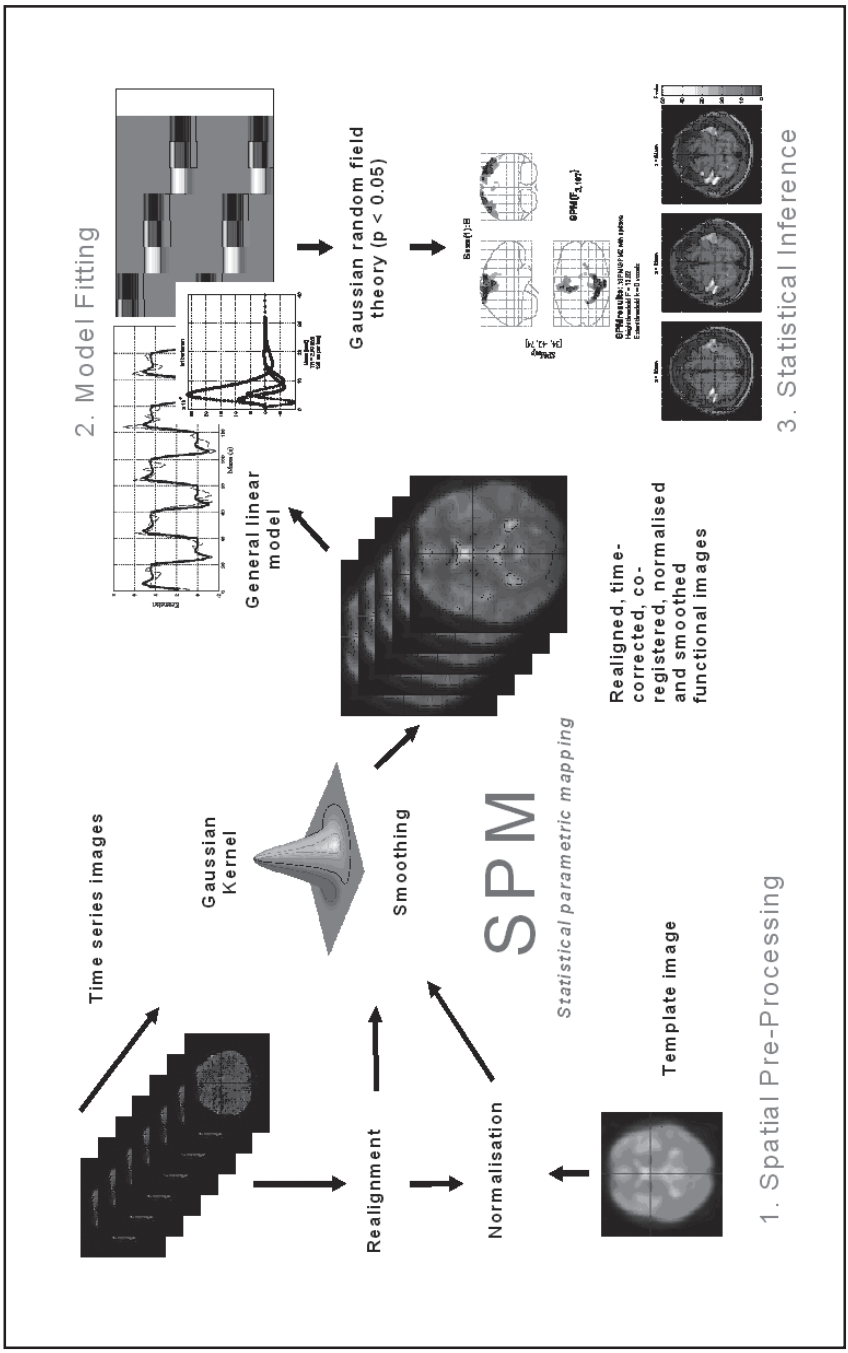

Figure 1. (b) Steps in fMRI data analysis using SPM2.

Post Processing of fMRI Data

All the functional (T2*-weighted) and structural (T1-weighted) images were sent to Universiti Kebangsaan Malaysia Hospital (HUKM) MedWeb and were later retrieved in the Medical Physics Laboratory, Diagnostic Imaging & Radiotherapy Programme, Faculty of Allied Health Sciences, UKM Kuala Lumpur for further analyses. Image analyses were performed using a personal computer with a high processing speed and large data storage. The MATLAB 6.5.0 (Mathworks Inc., Natick, MA, USA) and Statistical Parametric Mapping (SPM2) (Functional Imaging Laboratory, Wellcome Department of Imaging Neuroscience, Institute of Neurology, University College of London) software packages were used for these purposes. The raw data in DICOM (.dcm) format were transformed into Analyze (.hdr, .img) format by means of SPM2. Functional images in each measurement were realigned using the 6-parameter affine transformation in translational (x, y and z) and rotational (pitch, roll and yaw) directions to reduce artifacts from subject movement. The images were then time-correct using sinc interpolation to ensure that each measurement was subjected to the same time interval. After realigning the data, a mean image of the series was used to estimate some warping parameters that mapped it onto a template that already conform to a standard anatomical space (EPI template provided by the Montreal Neurological Institute). [17] The normalisation procedure used a 12-parameter affine transformation where the parameters constituted a spatial transformation matrix. [18] The images were then smoothed using a 6-mm full-width-at-half-maximum (FWHM) Gaussian kernel. Activated voxels were identified by the general linear model approach by estimating the parameters of the model and by deriving the appropriate test statistic (T-or F-statistic) at every voxel. Statistical inferences were finally obtained on the basis of SPM and the Gaussian random field theory. [17] Fig. 1(b) shows all the steps taken in data analyses using SPM.

RESULTS AND DISCUSSION

In this study, the response variables in motor cortices due to finger movements were observed for Y_j measurements where $j = 1 - J$, indexes the observations. For each observation, a set of L ($L < J$) explanatory variables denoted by x_{jl} were obtained where $l = 1 - L$, indexes the explanatory variables. A general linear model that explains the response variable Y_j in terms of a linear combination of the explanatory variables plus an error term, can thus be written as [19]

$$Y_j = x_{j1}\beta_1 + \ldots + x_{jl}\beta_l + \ldots + x_{jL}\beta_L + \varepsilon_j. \quad (1)$$

β_l is unknown parameter corresponding to each of the L explanatory variables x_{jl}. The errors ε_j are independent and identically distributed (i.i.d.) normal random variables with zero mean and variance σ^2 which is written as $\varepsilon_j \sim N(0, \sigma^2)$. For each observation $j = 1 - J$ and for β_l with $l = 1 - 4$, the general linear model can be written in full as

$$
\begin{aligned}
Y_1 &= x_{11}\beta_1 + x_{12}\beta_2 + x_{13}\beta_3 + x_{14}\beta_4 + \varepsilon \\
&\vdots \\
Y_j &= x_{j1}\beta_1 + x_{j2}\beta_2 + x_{j3}\beta_3 + x_{j4}\beta_4 + \varepsilon \\
&\vdots \\
Y_J &= x_{J1}\beta_1 + x_{J2}\beta_2 + x_{J3}\beta_3 + x_{J4}\beta_4 + \varepsilon
\end{aligned}
\tag{2}
$$

The parameters β_1, β_2, β_3 and β_4 correspond namely to the explanatory variables for UNI_{right}, UNI_{left}, BIM and baseline responses respectively. Eqn. (1) and Eqn.(2) clearly denote that Y is the measured time series data of length J at a given location (voxel) in the brain. In this study, J or the number of measurements is 120. Eqn. (2) can be rewritten in matrix form of

$$
\begin{pmatrix} Y_1 \\ \vdots \\ Y_j \\ \vdots \\ Y_J \end{pmatrix} = \begin{pmatrix} x_{11} & x_{12} & x_{13} & x_{14} \\ \vdots & \vdots & \vdots & \vdots \\ x_{j1} & x_{j2} & x_{j3} & x_{j4} \\ \vdots & \vdots & \vdots & \vdots \\ x_{J1} & x_{J2} & x_{J3} & x_{J4} \end{pmatrix} \begin{pmatrix} \beta_1 \\ \beta_2 \\ \beta_3 \\ \beta_4 \end{pmatrix} + \begin{pmatrix} \varepsilon_1 \\ \vdots \\ \varepsilon_j \\ \vdots \\ \varepsilon_J \end{pmatrix}
\tag{3}
$$

Eqn. (3) in matrix notation is then

$$Y = X\beta + \varepsilon \tag{4}$$

In Eqn. (4), Y is the column vector of observations, ε the column vector of error terms and β the column vector of parameters β_1, β_2, β_3 and β_4. X is the designed matrix of dimension (J,4) which contains the effects that influence the measured signal, for example, signals from UNI_{right}, UNI_{left} or BIM. It is also called the (J,4) matrix of regressors. Given Y and X, the parameters β_1, β_2, β_3 and β_4 can be estimated using least-square method.[19] The general linear model used is said to have four conditions which correspond namely to UNI_{right}, UNI_{left} or BIM coordinations of movement. The fourth condition is for the baseline. The schematic representation of the general linear model and the corresponding designed matrix are shown in *Figs. 2(a)* and *(b)* respectively. The model used in this study supposes that the shape of the hemodynamic response function (HRF) can be approximated by a canonical HRF as given by *Fig. 2(c)*.[20] With reference to *Fig 2(a)* and *(b),* the model consists of a set of assumptions. The voxels that are active during UNI_{right} might have time series as shown by A. Voxels that are active during UNI_{left} might have time series as shown

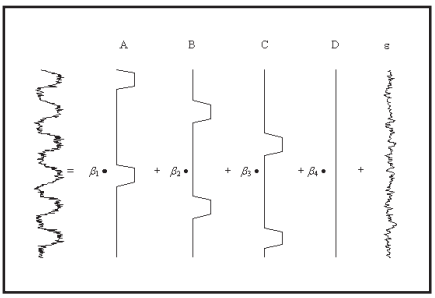

Figure 2. (a) The general linear model

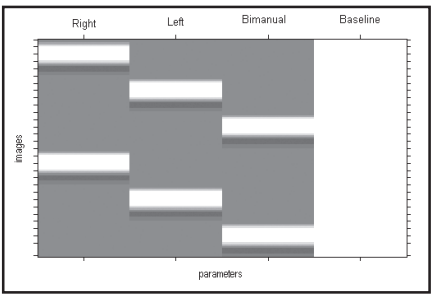

Figure 2. (b) Designed matrix for the T-contrast

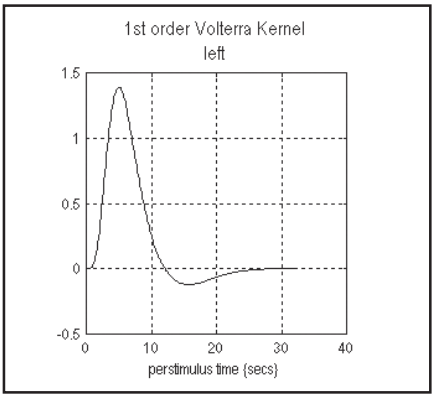

Figure 2. (c) The canonical HRF used in this study

by B. Voxels that are active during BIM might have a time series as shown by C and for voxels that just do nothing throughout the whole scan might have time series that looks like D. For a given voxel, the general linear model, by means of least square fitting, will figure out just what type that voxel is by modelling it as a linear combination of the hypothetical time series, as mentioned earlier .[19] The fitting or estimation entails finding the parameter values (β_1, β_2, β_3 and β_4) such that the linear combination best fits the measured data. These conclude that the same general linear model can be used for all voxels but with different set of parameters for each voxel.

Figs. 3(a, c, e and g) are the glass images or the maximum intensity projection (MIP) of the brain in neurological appearance (the left side of the image is the actual left side of the subject) showing the effects of interest and the activation that exist during UNI_{right}, UNI_{left} or BIM. *Figs. 3(b, d, f and h)* show the corresponding designed matrix and contrast vector used to produce the images. The images were obtained from SPM analysis on each voxel using the *T* contrast, SPM {T} and were displayed based on the Tailairach & Tournoux coordinates. [21] The *t* value for each time series voxel for the *T*-contrast image is calculated from the relation. [22]

$$t = [c^T\beta]/[\sigma(c^T(X^TX)^{-1}c)^{1/2}] \quad (5)$$

where c is the weight of the parameter estimates used to form the numerator of the statistics, c^T is the transposed matrix of c, β is the parameter model to be estimated (i.e. β_1, β_2, β_3 and β_4), σ is the standard deviation and X and X^T is the designed matrix and its transposition respectively. c is actually a vector or matrix that contains the contrasts weights. In other words, the t-value is the contrast of the estimated parameters devided by the square root of the variance estimate. The contrast weights must be specified to define the contrast which is written as $c^T\beta$. To get all the effects of interest from all conditions that are different from the baseline, the matrix c^T is [1 1 1 0], as can be seen in *Fig. 3(b)*. This will gives all the time series voxels that are active during UNI_{right}, UNI_{left} or BIM, as compared to the baseline. The shadowed regions or blobs on the MIPs represent the statistical image of the effects of interest obtained from the application of t-test on each voxel and by correcting the p value using the Family Wise Error (FWE) method at $p = 0.05$. Clusters that contain numbers of voxel equal or less than 10 are thresholded. With FWE ($p = 0.05$), only one false positive is expected in 20 statistical parametric maps produced. A comprehensive discussion on the Gaussian random field theory has been given elsewhere. [23] The darker the voxel, the higher the intensity of the signal. The cut-off t-value is 5.19 which means that voxel with t-value lower than the cut-off value will not be shown as being active. Maximum signal intensity occurred at Talairach & Tournox coordinates of (38, -36, 72) which is on the right hemisphere.

To test for any activation due UNI_{right} only, the matrix c^T is taken as [1 0 0 0]. The MIPs and the designed matrix with the corresponding contrast vector are given in *Fig. 3(c)* and *(d)*. The t-value used for the t-test is again 5.19. The MIPs is thresholded for clusters with number of voxels equal to or less than 10. It can be seen that the activated region is found to be on the motor area of the left hemisphere of the brain. The maximum signal intensity is found to be at coordinates (-36, -14, 52). The number of activated voxel in the main cluster searched by SPM around the coordinates (-36, -14, 52) are 477.

To test for any activation for UNI_{left}, the contrast vector used is [0 1 0 0]. *Fig 3(e)* and (f) show the activations and the corresponding designed matrices. The activated brain region during the left hand finger movement is found to be in the motor area of the right hemisphere. The threshold t-value used for the t-test is also 5.19. The maximum signal intensity for the left hand finger movement occurred at coordinates (36, - 40, 72). By considering only clusters with number of voxels larger than 10, the number of activated voxels in the main clusters searched by the SPM around the coordinates of maximum intensity (36, -40, 72) are 869. This is about twice the number of activated voxels in the left hemisphere for UNI_{right} obtained from the same search volume.

Brain activation during BIM is shown in *Fig. 3(g)* with the corresponding design matrix in *Fig. 3(h)*. The contrast vector used was [0 0 1 0]. The MIPs were produced via FWE ($p = 0.05$) with the height threshold taken as $t = 5.19$. It is evident that the intensity of the brain activations are much more pronounced on the motor area in the right hemisphere from BIM_{left} as compared to the activations for BIM_{right} in the left hemisphere. By considering only clusters with number of voxels larger than 10, the activation area (number of voxels in the main cluster) on the right hemisphere was also found to be higher (1192 voxels) then on the left hemisphere (289 voxels). However, the point of maximum intensity is shifted to new coordinates of (38, -

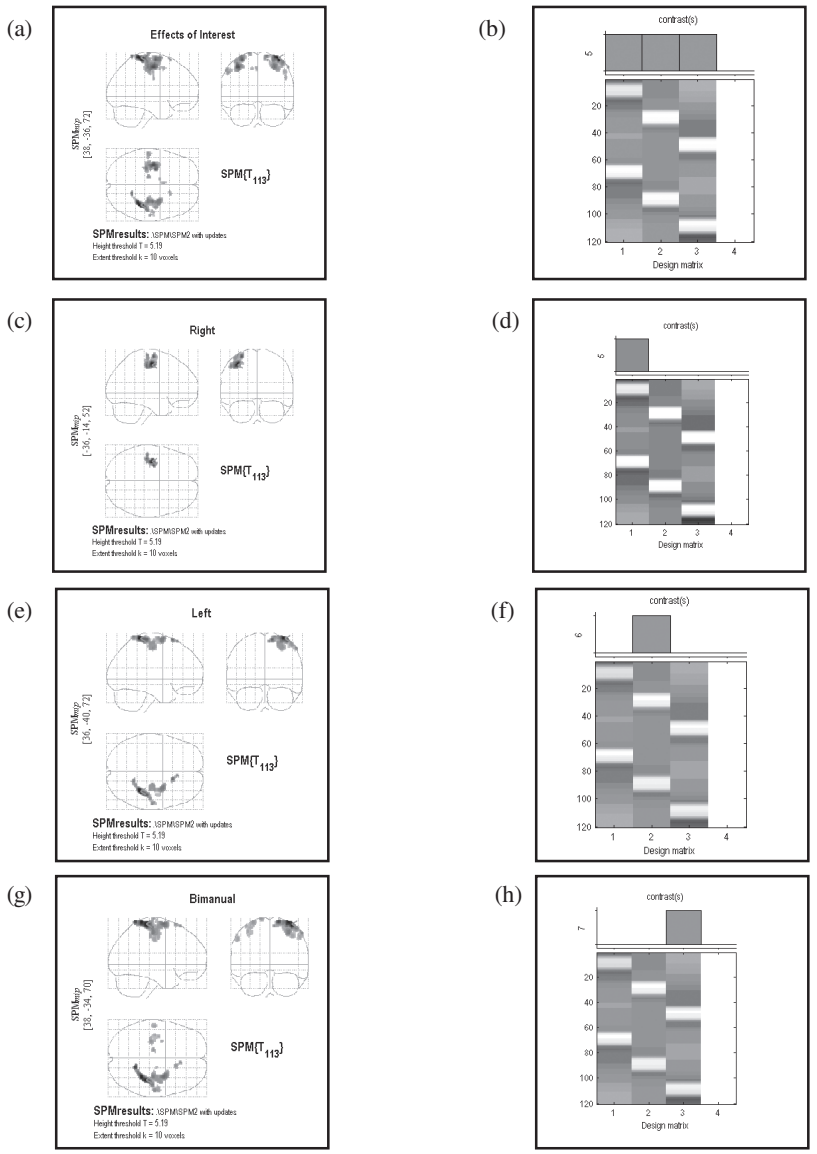

Figure 3. The maximum intensity projection (MIP) or glass images for the effects of interest, UNI_{right}, UNI_{left} and BIM with their respective designed matrix and contrast vectors for *T*-contrast

34, 70) but still in the vicinity of the maximum intensity for UNI_{left}. Plots of the predicted hemodynamic response at the point of maximum intensity for all finger movements are shown in *Fig. 4*. The values confirmed the fact that a higher signal intensity is produced for UNI_{left} as compared to UNI_{right}. For BIM, a higher signal intensity is observed in the right hemisphere (due to BIM_{left}), almost similar to that produced by UNI_{left}.

The results show that, the activated brain regions due to the self-paced finger movements are on the precentral and postcentral gyrii covering the primary motor and somatosensory primer areas. Contralaterality can be clearly observed for UNI_{right} and UNI_{left}. The primary somatosensory areas which are located directly posterior to the central sulcus of each cerebral hemisphere receive nerve impulses for touch during the experiment, while the primary motor areas which are located in the precentral gyrus of the frontal lobe controls voluntary contraction during finger movements. A considerably large area of activations observed in this study is due to a large number of receptors present in the fingertips since more cortical areas are devoted to those muscles involved in skilled and delicate movement. [24] It is evident that for both UNI and BIM, the activation is larger and stronger on the right hemisphere where the maximum intensity is shown by a voxel at coordinates (38, -34, 70). The results support the fact that for a right-handed person, the activated motor area on the right hemisphere of the brain during UNI_{left} experienced a higher and larger coverage of hemodynamic response compared to the left hemisphere of the brain during UNI_{right}.

A simple extension of the model in *Fig. 2(a)* is given in matrix form in Eqn. (6) and in the designed matrix representation in *Fig. 5(a)*. Each condition is now modeled with three basis functions namely the canonical HRF and its temporal and dispersion derivatives. The peristimulus basis set of the canonical HRF and its derivatives are depicted in *Fig. 5(b)*. These functions are able to model the HRF as well as its delay and dispersion. The temporal derivative has been shown to be able to capture differences in the latency of the peak response while the dispersion derivative determines the duration of the peak response. [20] The designed matrix is accompanied (on the top) by the selected contrasts which were chosen to produce the effects of interest that can be obtained from the whole finger tapping experiment. A detailed discussion on contrast and classical inference has been given by Poline *et al.* [22] but will also be discussed in the following paragraphs. Specifically, the first, fourth and seventh columns of the designed matrix separately modeled the hemodynamic responses for UNI_{right}, UNI_{left} and BIM respectively. The second, fifth and eighth columns are the time derivatives for the first, second and third condition and the third, sixth and ninth column representing the dispersion derivative of the canonical HRF for each condition. The final or the tenth column is dedicated to the baseline. Brain activations due to UNI and BIM will be further discussed based the *F*–statistic or SPM{F}.

$$\begin{pmatrix} Y_1 \\ \vdots \\ Y_j \\ \vdots \\ Y_J \end{pmatrix} = \begin{pmatrix} x_{11} & \dots x_{1L} \dots & x_{10} \\ \vdots & & \\ x_{j1} & \dots x_{2L} \dots & x_{j10} \\ \vdots & & \\ x_{J1} & \dots x_{JL} \dots & x_{J10} \end{pmatrix} \begin{pmatrix} \beta_1 \\ \beta_2 \\ \beta_3 \\ \beta_4 \\ \beta_5 \\ \beta_6 \\ \beta_7 \\ \beta_8 \\ \beta_9 \\ \beta_{10} \end{pmatrix} + \begin{pmatrix} \varepsilon_1 \\ \vdots \\ \varepsilon_j \\ \vdots \\ \varepsilon_J \end{pmatrix} \quad (6)$$

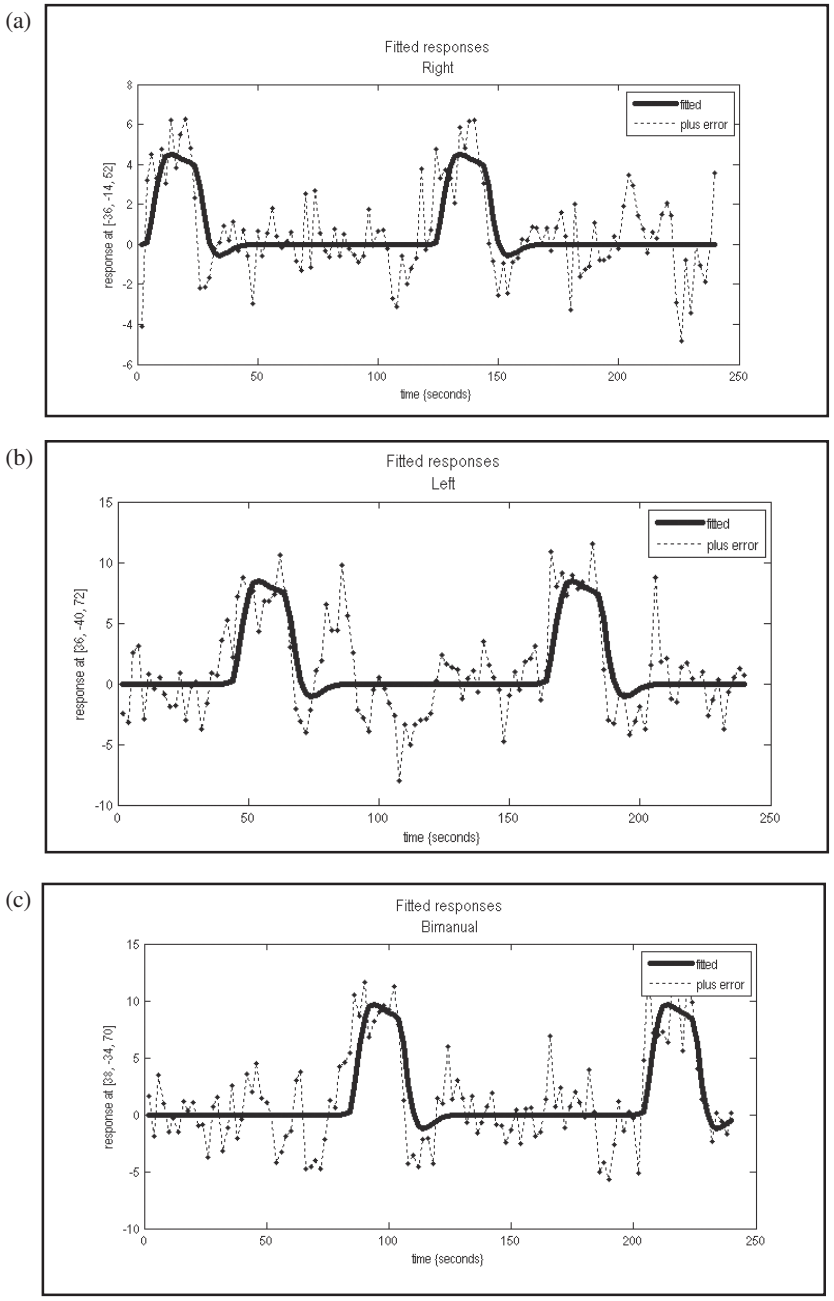

Figure 4. The hemodynamic response function for (a) UNI_{right}; (b) UNI_{left} and; (c) BIM measured at the point of maximum intensity on the *T*-contrast MIPs

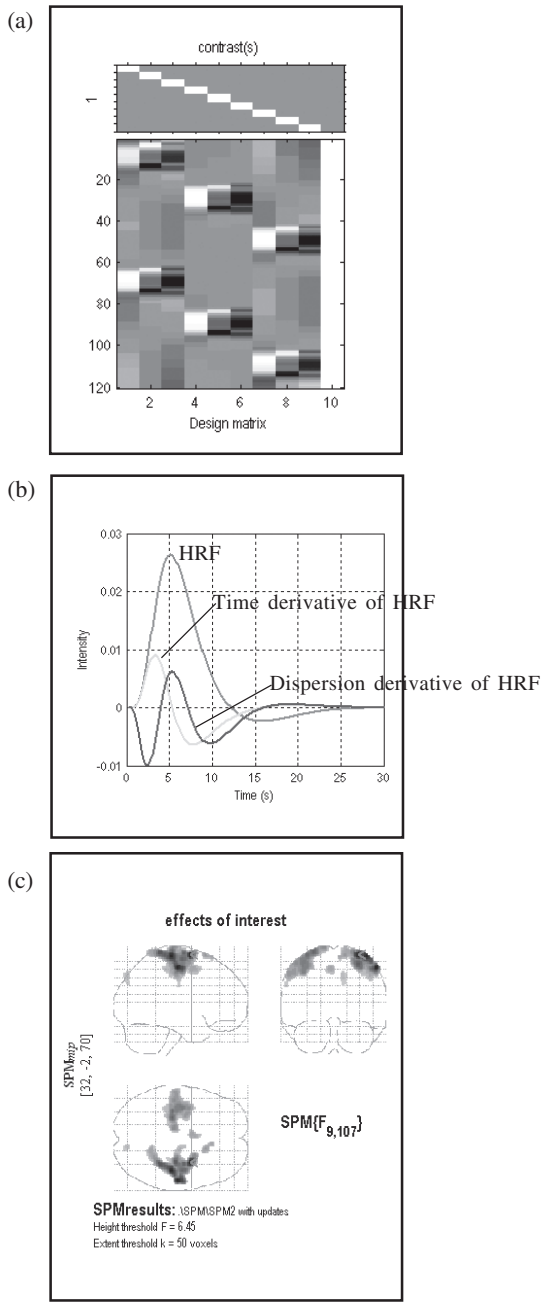

Figure 5. **(a)** The designed matrix and contrast vectors for an *F*-contrast; (b) canonical HRF with its time and dispersion derivatives; and (c) the MIPs for the observed effects of interest obtained from an *F*-contrast.

As mentioned earlier, the MIPs in *Fig. 5(c)* show all the effects of interest from the finger tapping experiment which have been obtained by applying the contrast vector (shown below in matrix form) onto the designed matrix *(Fig. 5(a))*.

$$\begin{pmatrix} 1000000000 \\ 0100000000 \\ 0010000000 \\ 0001000000 \\ 0000100000 \\ 0000010000 \\ 0000001000 \\ 0000000100 \\ 0000000010 \end{pmatrix}$$

It can be clearly seen that the activation areas are larger than that shown by *Fig. 3(a)*. The contrast vector shown above reflects the use of the *F*-statistic in the analysis. The *F*-value of 6.45 depicted in the figure is the ratio of the two S squares (the estimation of the population variance) calculated for all voxels across the whole brain volume. The corresponding mathematical relation is simply

$$F_{\text{df} = (\text{K-1}),\ \text{K(n} - 1)} = [nS_{X'}^2/ave.\ S_X^2] \tag{7}$$

with *df* = degree of freedom, *K* = number of random samples of *n* items and $nS_{X'}^2$ is an estimate of the population variance and

$$nS_{X'}^2 = \Sigma(X - X'')^2/(K - 1) \tag{8}$$

with X'' is the mean of the *K* means. The ave.S_X^2 is the average of the S_X^2's of the *K* samples with the estimate of the population variance S_X^2 can be written as

$$S_X^2 = \Sigma(X - X')^2/(n - 1) \tag{9}$$

where X' is the mean of a random sample of n items. Eqn. (7) in SPM language is simply the ratio between the additional variance accounted for by tested effects and the error variance estimate.

Fig. 6(a – c) represent MIPs and the corresponding contrast and designed matrix for the activations obtained from $\text{UNI}_{\text{right}}$, UNI_{left} and BIM via an *F*-contrast analysis. The *p* value is corrected using the Family Wise Error (FWE) method at $p = 0.05$ and only clusters with number of voxels larger than 10 are considered. The hemispherical side of activations are in good agreement with that obtained from the *T* contrast analysis. Contralaterality can be clearly observed for $\text{UNI}_{\text{right}}$ and UNI_{left} while the brain activation is larger in the right hemisphere than in the left hemisphere for BIM.

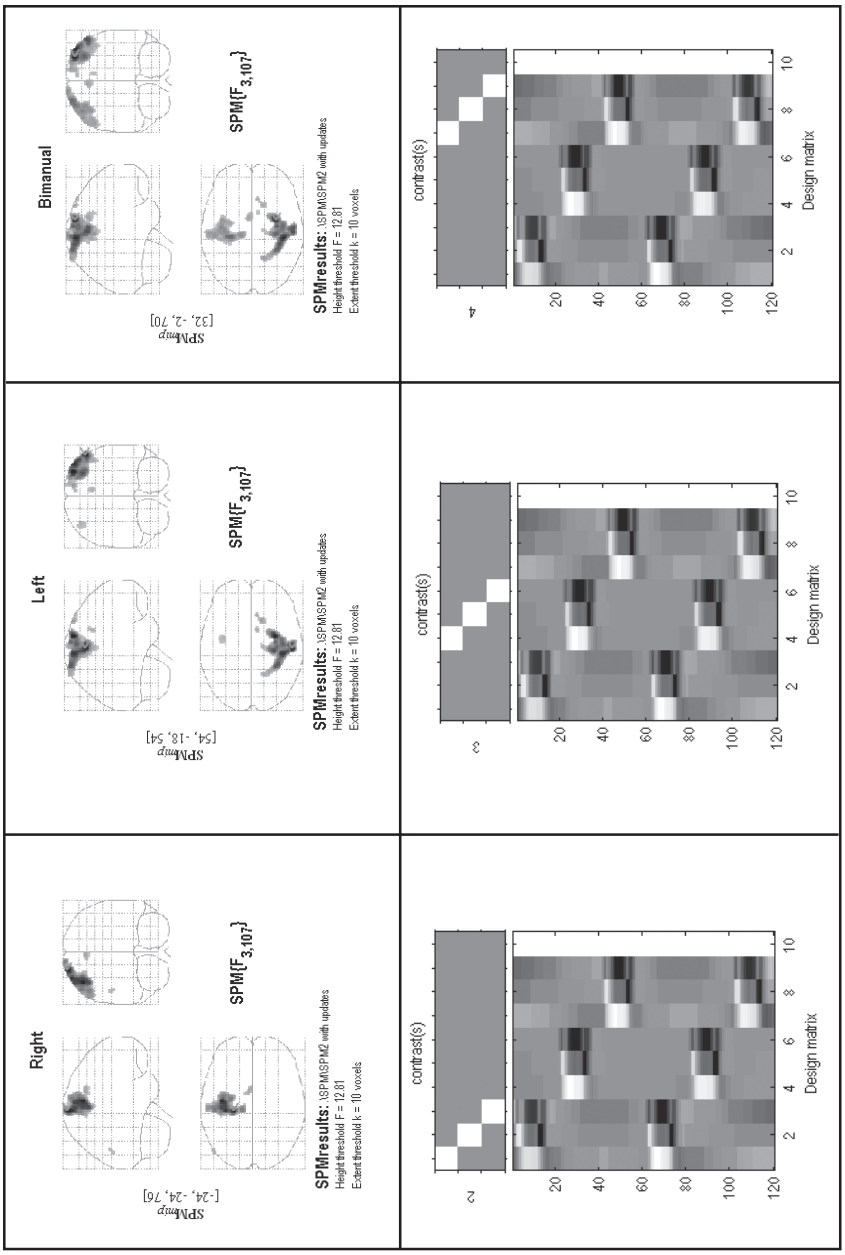

Figure 6. The maximum intensity projection (MIP) or glass images for (a) UNI_{right}, (b) UNI_{left} and (c) BIM, with their respective designed matrix and contrast vectors for an *F*-contrast.

The area of activations are much larger than that shown by *Fig. 3(c), 3(e) and 3(g).* This could be due to the ability of the *F* contrast analysis to capture the magnitude of the HRF as well as its time and dispersion derivatives for a single voxel. The number of activated voxels searched in the largest cluster for UNI_{right} (in the left hemisphere) is found to be 1581 while for UNI_{left} (in the right hemisphere), the result indicates 1951 activated voxels. For BIM, the number of activated voxels in the right hemisphere searched over the largest cluster of activation are 1873 while in the left hemisphere, there are only 1374 voxels that are activated in the largest cluster. The results show an unequal number of activated voxels in the right and left hemispheres during the UNI and BIM tasks. However, it is hypothesised that the number of activated voxels in both the left and right hemispheres during BIM could equal the number of activated voxels in the respective right and left hemispheres during UNI if the subject taps his finger at a consistent pace by pressing against the thumb with the same magnitude of force. A detailed study on these is still being conducted.

The signal measured at the point of maximum intensity (global maximum) which occurs at coordinates (-24, -24, 76), (54, -18, 54) and (32, -2, 70) for the UNI_{right}, UNI_{left} and BIM is on average higher than that obtained from the *T*-contrast. The coordinates for the point of maximum intensity for UNI_{left} and BIM are no longer the same. The predicted hemodynamic response function for all types of movements are shown in *Fig. 7*. The plots show a significant difference ($p< 0.05$) between the active and resting state, rejecting the null hypothesis of no difference imposed earlier. Unlike the plots in *Fig. 4*, the hemodynamic response depicted in *Fig. 7* is characterised by an initial sharp spike before residing into a plateau at the end of the response. The negative undershoot in Fig. 7 is also relatively higher in magnitude than that shown in *Fig. 4.* The underlying mechanism that governs the occurrence of the sharp spike and undershoot in *Fig. 7* is unknown, and needs further attention. Regardless of the sharp peak, the intensity of the response measured at the point of maximum intensity in the right hemisphere (UNI_{left}) is about the same with that in the left hemisphere (UNI_{right}), while the HRF peak for BIM is higher than the UNI_{right} and UNI_{left}. These results are in agreement with the results obtained via the *T*-test.

Fig. 8(a – c) represent BOLD statistical images obtained from SPM{F} which are overlaid onto several axial T1 weighted images of the same level (z coordinates) that correspond to UNI_{right}, UNI_{left} and BIM. The images are in radiological appearance (the left side of the image is the actual right side of the subject). The magnitude of the activations (the intensity of the hemodynamic response) thresholded using the *F*-values are colour coded as shown on the right side of the images. The ipsilateral activation in the left hemisphere for UNI_{left} can be clearly seen in *Fig. 8(b).*

As mentioned earlier, the number of activated voxels in the right or left hemispheres during UNI_{right} and UNI_{left} do not equal the number of activated voxels in the respective right or left hemispheres involved in BIM ($N_{unileft} \neq N_{bimleft}$, $N_{uniright} \neq N_{bimright}$). Furthermore, in both UNI and BIM, the left and right hemispheres show an unequal number of activated voxels ($N_{leftuni} \neq N_{rightuni}$, $N_{leftbim} \neq N_{rightbim}$). Despite the fact that this is caused by inconsistent tapping pace and force, it could also indicate an asymmetry of neuro transmission that goes along in the subject. Further analyses performed on these hemispherical activations

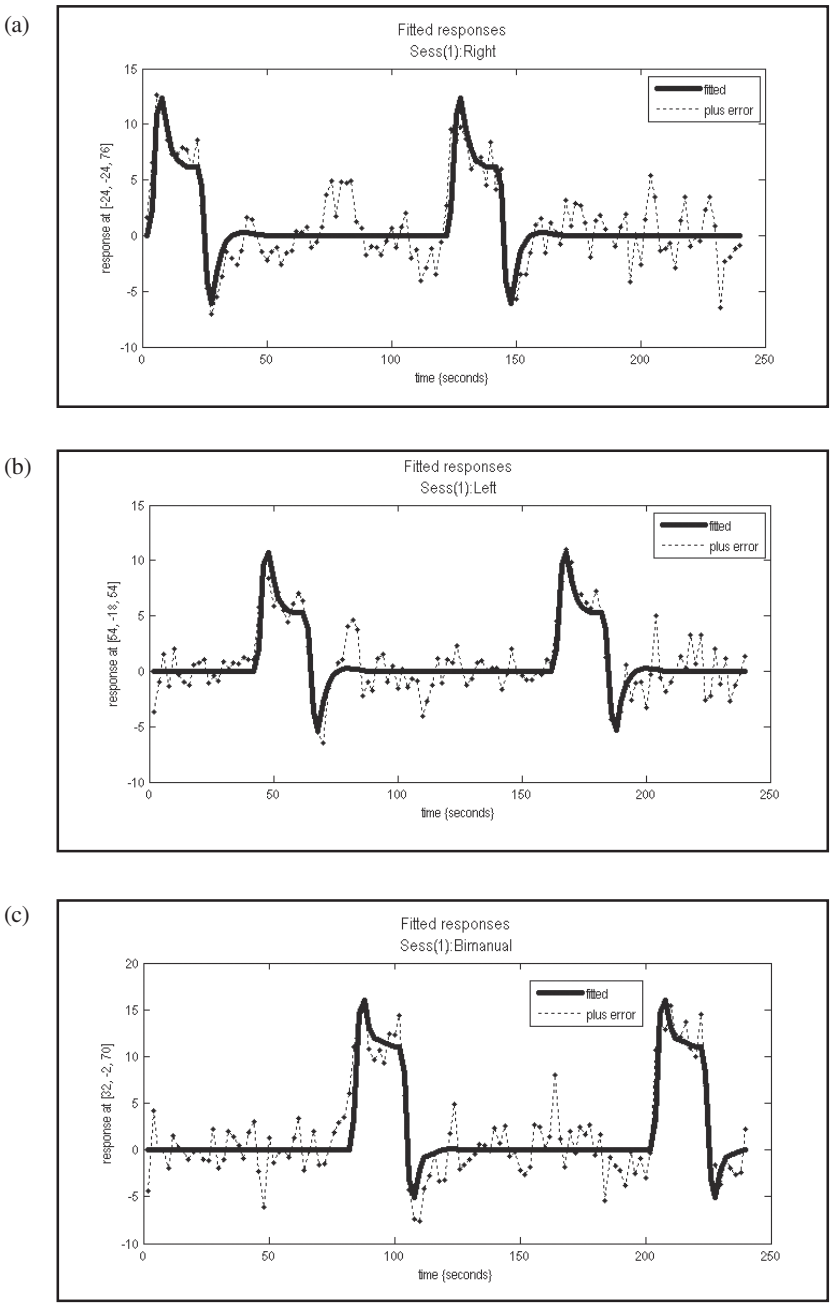

Figure 7. The hemodynamic response function for (a) UNI_{right}, (b) UNI_{left} and (c) BIM measured at the point of maximum intensity on the *F*-contrast MIPs.

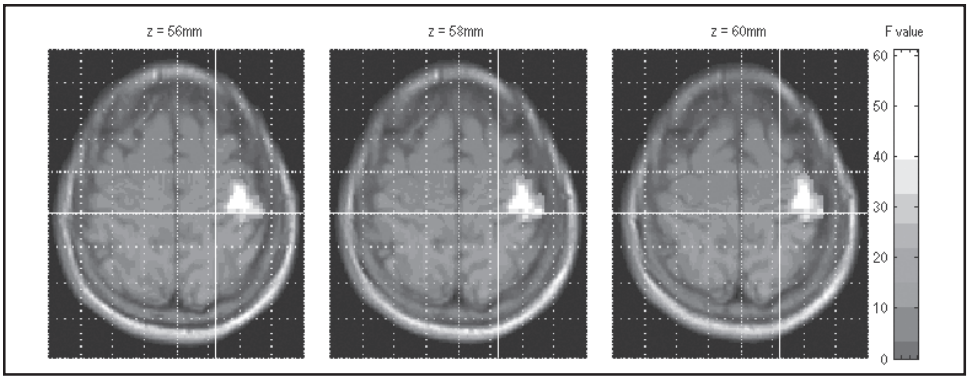

(a)

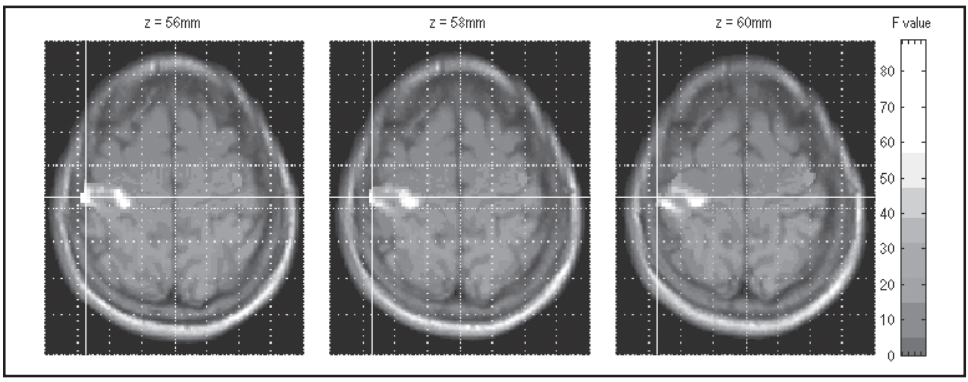

(b)

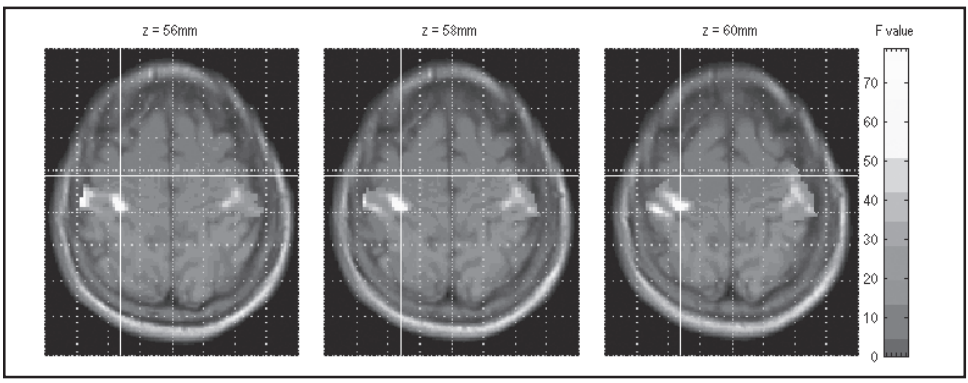

(c)

Figure 8. Brain activation in the motor cortices for (a) UNI_{right}, (b) UNI_{left} and (c) BIM observed on the same z position.

yielded an interesting kind of functional connectivity between the two hemispheres during BIM. This is obtained by initially applying the contrast vector (shown below) onto the designed matrix.

$$\begin{pmatrix} 000100\text{-}1000 \\ 0000100\text{-}100 \\ 00000100\text{-}10 \end{pmatrix}$$

This operation is to test the question of "Is there any difference between the number of activated voxels that are involved in UNI_{left} and BIM ?". The fact, that the answer to the question is the activated voxels in the left hemisphere is expected since BIM has brain activations on both hemispheres while for UNI_{left}, the activation occurs only in the right hemisphere. Furthermore, the number of activated voxels in UNI_{left} is larger than in BIM_{left}. The results are depicted in *Fig. 9(a)* which show the MIPs of the activated voxels in the left hemisphere and the corresponding designed matrix and contrast vector. However, the number of activated voxels calculated from the images are 468 only, whereas the number of activated voxels for BIM_{right} which has been obtained earlier is 1374. This indicates that (1374 – 468) = 906 voxels which are active for BIM_{right} are now missing.

To test for any different in number of voxels involved in UNI_{right} and BIM, the contrast vector used are as follows:

$$\begin{pmatrix} 100000\text{-}1000 \\ 0100000\text{-}100 \\ 00100000\text{-}10 \end{pmatrix}$$

What is expected from the contrast vector above is that it will give brain activation in the right hemisphere in accordance with UNI_{left} since the number of voxels for UNI_{right} is larger than for BIM_{right}. As can be seen in *Fig. 9(b)*, the resulting brain activations are clustered in the right hemisphere but with less number of voxels when compared to activation in the right hemisphere during BIM. The number of activated voxels is 937 whereas the number of activated voxels during BIM_{left} in the right hemisphere which has been obtained earlier is 1873. This indicates that (1873 – 937) = 936 voxels in the right hemisphere which are activated during BIM are now hibernating. These findings will be discussed based on functional connectivity as follows.

The occurrence of missing voxels in both cases indicates the existence of functional connectivity during BIM. The results from the analyses above suggest that all the activated voxels during BIM in both hemispheres are involved in the respective UNI_{right} or UNI_{left}. It is also believed that all the missing voxels in the above mentioned cases are functionally connected to the voxels in the opposite hemisphere. For example, when all the voxels that are responsible for UNI_{right} (in the left hemisphere) are deactivated from the MIPs for BIM by comparing the UNI_{right} and BIM responses, the voxels in the right hemisphere which are functionally connected with the deactivated voxels in the left hemisphere are also de-activated and do not appear on the MIPs resulting in less number of activated voxels in the right hemisphere. Similarly, when all the voxels that are responsible for UNI_{left} (in the right hemisphere) are deactivated from the MIPs of BIM by comparing the UNI_{left} and BIM

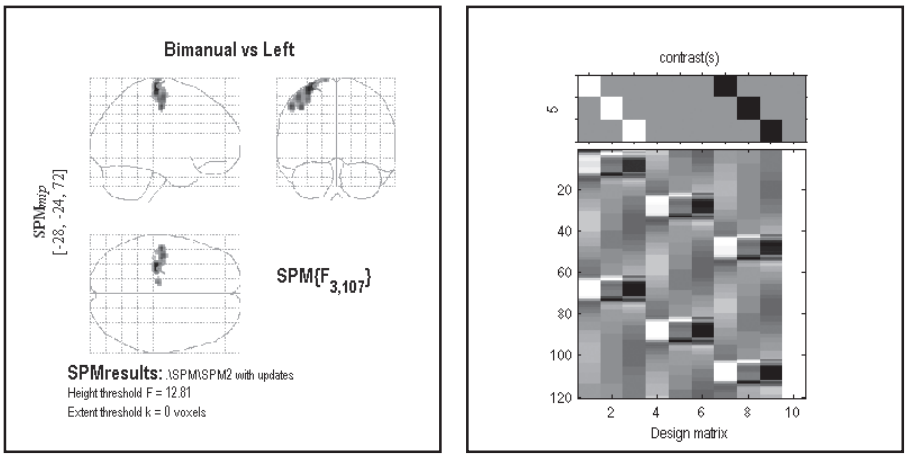

(a)

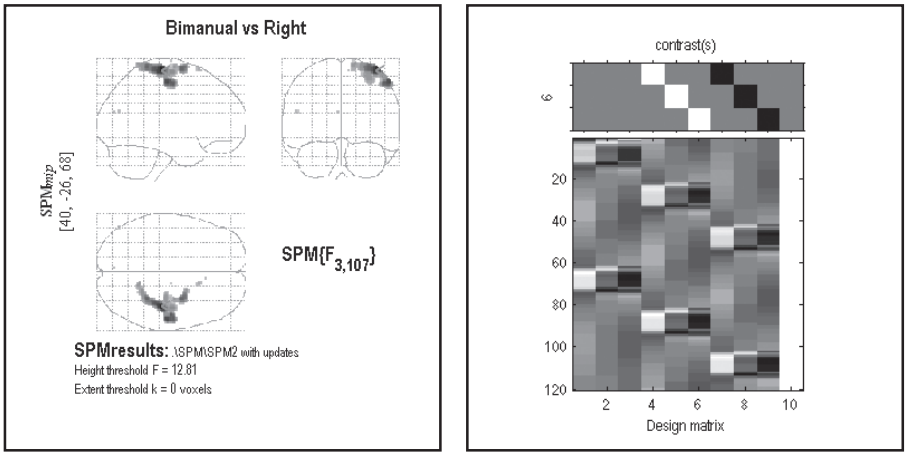

(b)

Figure 9. The occurrence of missing voxels in the MIPs shown in the (a) right hemisphere and (b) left hemisphere indicates an interhemispheric connectivity during BIM.

responses, the voxels in the left hemisphere which are functionally connected with the deactivated voxels in the right hemisphere disappear and do not appear on the MIPs resulting in less number of activated voxels in the left hemisphere. These findings can be used to determine the existence of neurotransmission exchange between the two hemispheres. However, a multiple subject study on the left- and right-handed subjects need to be conducted to clarify the underlying phenomena of the interhemispheric connection during the bimanual type of movement. Table 1 summarises all the analyses done on the data.

Table 1. Number of contra-and ispilaterally activated voxels obtained from SPM{F} analyses; hight threshold (F) = 12.81, extent threshold (k) = 10 voxels, corrected p value = 0.05 (FWE).

Type of movement	Side of brain that is activated	Number of activated voxel	Talairach & Tournoux coordinates of maximum signal intensity	Number of activated voxel on the hemisphere that is ipsilateral to the side of movement
UNI_{right}	Left hemisphere	1581	-24, -24, 76	0
UNI_{left}	Right hemisphere	1951	34, -40, 72	70
BIM_{right}	Left hemisphere	1374	-32, -24, 70	* 906 (right hemisphere)
BIM_{left}	Right hemisphere	1873	34, -42, 74	*936 (left hemisphere)

* denotes number of missing voxels as explained in the text.

The brain activation observed in this study reflects the increase in the magnetic resonance signal intensity when the subject moves his fingers. This is attributed to an increase in the concentration of the diamagnetic oxyhemoglobin in venous blood (decrease in the deoxyhemoglobin content) in the brain. This phenomena has been discussed as occuring due to an increase in the cerebral blood flow (CBF) in a particular part of the brain, for example, the primary and supplementary motor areas that control finger movement.[25, 26] As a result, the supply of oxygen to those areas exceeds the demand and the oxygenated blood will eventually increase the magnetic field homogeneity due to the diamagnetic property of the oxyhemoglobin. The increase in the localised magnetic field homogeneity would increase the T2* relaxation time of the tissues and their surroundings, hence an overall increase in the magnetic resonance signal intensity[27] measured on a T2*-curve. The oxyhemoglobin is said to act as an endogenous contrast medium which enables the differentiation between the activated and nonactivated tissues on magnetic resonance images.[28] This is possible because diamagnetic oxyhemoglobin and paramagnetic deoxyhemoglobin possess different magnetic susceptibility values.[29] This behaviour is similar to the change in the magnetic properties shown by the tissues after the administration of paramagnetic exogenous contrast media. The dependence of the magnetic resonance signal intensity on blood oxygenation has been reported in several earlier works [4,5,6] and the mechanisms underlying the changes in the signal intensity have been thoroughly discussed and proposed.[30] To date, the exact mechanism of BOLD still remains complex, serving as an area of interest for those working in this field.

Finally, as elaborated by Friston [17], the implementation of statistical analysis to make inferences about the data, given the effect is zero in this single-subject study, represents a fixed-effect or first level analysis where the error variance is estimated on a scan-to scan basis, assuming that each scan represents an independent observation (ignoring serial correlation). In other words, inferences were made about the data that have been obtained only from a single subject. However, the scan-to-scan error variance is not necessarily

appropriate for inference about group responses. In order to infer that a group of subjects show significant activation, the variability in activation effects must be assessed from subject to subject. The variability now constitutes the proper error variance.[17] This second-level analysis is referred to as random-effects analysis. A further study on the response of the human brain to the movement of hand fingers using random-effects analysis is necessary in order to make appropriate inferences about group responses.

CONCLUSION

The hemodynamic response function in the cerebral cortices due to the BOLD mechanism can be studied and evaluated using functional magnetic resonance imaging technique and statistical parametric mapping. Brain activations obtained via the *F*-test indicate a uniform and larger activation area compared to that obtained from the *T*-test. The results show that the activated brain regions due to the self-paced finger movements are the precentral and postcentral gyrii covering the primary motor, premotor and somatosensory primer areas. The active-state signal intensity was found to be significantly higher than that of the resting-state. For UNI, brain activations showed contralaterality with a higher intensity and area of activation for UNI_{left}. Small ipsilateral activation was observed during UNI_{right} and UNI_{left}. For BIM, the activation was observed in both hemispheres with the right hemisphere showing a higher signal intensity and coverage. The results support the fact that for a right-handed person performing a bimanual type of movement, the activated motor areas on the right hemisphere of the brain during UNI_{left} experienced a higher intensity and larger coverage of hemodynamic response compared to the left hemisphere of the brain during UNI_{right}. Analyses performed on the activated regions of interest (ROI) by comparing the unimanual and bimanual types of activations revealed that during BIM, there are voxels in the left hemisphere controlling the movement of the left hand fingers and voxels in the right hemisphere controlling the movement of the right hand fingers. The ipsi- and contra-lateral type of activations observed in this study resemble the existence of functional specialisation and connectivity in cerebral motor cortices within and in between both hemispheres. A further study on motor activation in human brain due to finger tapping stimulus is necessary in order to have a clearer view on the mechanism that governs interhemispheric connection.

ACKNOWLEDGEMENT

The authors would like to thank Sa'adon Samian and Mazli Mohd Zin from the Department of Radiology, Universiti Kebangsaan Malaysia Hospital for the fMRI scans and Jesper Andersson from KI, Stockholm & BRU, Helsinki for a fruitful discussion on experimental methods and the general linear model. This work is supported by the IRPA research grant 09-02-02-0119EA296 from the Ministry of Science, Technology and Innovation.

REFERENCES

[1] Buxton RB. Introduction to functional magnetic resonance imaging : principles and techniques. Cambridge : Cambridge University Press, 2002.

[2] Mansfield P. Multiplanar image formation using NMR spin echoes. J Phys C 1977; 10 : L55 – L58.

[3] Bernstein MA, King KF, Zhou XJ. Handbook of MRI pulse sequences. Burlington: Elsevier Academic Press, 2004.

[4] Ogawa S, Lee TM, Nayak AS *et al.* Oxygenation-sensitive contrast in magnetic resonance imaging of rodent brain at high magnetic fields. Magn Reson Med 1990; 14 : 68 – 78.

[5] Ogawa S, Lee TM. Magnetic resonance imaging of blood vessels at high fields : *in vivo* and *in vitro* measurements and image simulation. Magn Reson Med 1990; 16 : 9 – 18.

[6] Ogawa S, Lee TM, Kay AR *et al.* Brain magnetic resonance imaging with contrast dependent on blood oxygenation. Proc Natl Acad Sci USA 1990; 87 : 9868 – 9872.

[7] Jäncke L, Specht K, Mirzazade S *et al.* The effect of finger-movement speed of the dominant and the subdominant hand on cerebellar activation : a functional magnetic resonance imaging study. NeuroImage 1999; 9: 497 – 507.

[8] Scheffler K, Bilecen D, Schmid N *et al.* Auditory cortical responses in hearing subjects and unilateral deaf patients as detected by functional magnetic resonance imaging. Cerebral Cortex 1998; 8 : 156 – 163.

[9] Parkes LM, Fries P, Kerskens CM *et al.* Reduced BOLD response to periodic visual stimulation. NeuroImage 2004; 21: 236 – 243.

[10] Wheeler ME, Buckner RL. Functional-anatomic correlates of remembering and knowing. NeuroImage 2004; 4: 1337 – 1349.

[11] Just MA, Newman SD, Keller TA *et al.* Imagery in sentence comprehension : An fMRI study. NeuroImage 2004; 21: 112 – 124.

[12] Shah YB, Marsden CA. The application of functional magnetic resonance imaging to neuropharmacology. Current Opinion in Pharmacology 2004; 4: 1 – 5.

[13] Uludað K, Dubowitz DJ, Yoder EJ *et al*. Coupling of cerebral blood flow and oxygen consumption during physiological activation and deactivation measured with fMRI. Neuroimage 2004; 23: 148 – 155.

[14] Vaidya CJ, Austin G, Kirkorian G *et al*. Selective effects of methylphenidate in attention deficit hyperactivity disorder : a functional magnetic resonance study. Neurobiology 1998; 95 : 14494 – 14499.

[15] Sabbah P, Chassoux F, Leveque C *et al*. Functional MR imaging in assessment of language dominance in epileptic patients. NeuroImage 2003; 18: 460 – 467.

[16] Sturm W, Longoni F, Weis S *et al.* Functional reorganisation in patients with right hemisphere stroke after training of alertness : A longitudinal PET and fMRI study in eight cases. Neuropsychologia 2004; 42 : 434 – 450.

[17] Friston KJ. Experimental design and statistical parametric mapping. In : Frackowiak RSJ, Friston KJ, Frith CD, Dolan RJ, Price CJ, Zeki S, Ashburner J & Penny WD (eds.). Human brain function. Amsterdam : Elsevier Academic Press, 2004 : 599 – 632.

[18] Ashburner J, Friston KJ.Spatial normalisation using basis function. In : Frackowiak RSJ, Friston KJ, Frith CD, Dolan RJ, Price CJ, Zeki S, Ashburner J & Penny WD (eds.). Human brain function. Amsterdam : Elsevier Academic Press, 2004 : 655 – 672.

[19] Kiebel S, Holmes A. The general linear model. In : Frackowiak RSJ, Friston KJ, Frith CD, Dolan RJ, Price CJ, Zeki S, Ashburner J & Penny WD (eds.). Human brain function. Amsterdam : Elsevier Academic Press, 2004 : 725 – 760.

[20] Henson R. Analysis of fMRI time series. In : Frackowiak RSJ, Friston KJ, Frith CD, Dolan RJ, Price CJ, Zeki S, Ashburner J and Penny WD (eds.). Human brain function. Amsterdam : Elsevier Academic Press, 2004 : 793 – 822.

[21] Kochunov P, Uecker A. Talairach Deamon Client version 2.0, The Research Imaging Center, UTHSCSA, *http://ric.uthscsa.edu/resources* 2003.

[22] Poline JB, Kherif F, Penny W. Contrasts and classical inference. In : Frackowiak RSJ, Friston KJ, Frith CD, Dolan RJ, Price CJ, Zeki S, Ashburner J and Penny WD (eds.). Human brain function. Amsterdam : Elsevier Academic Press, 2004 : 761 – 779.

[23] Brett M, Penny W, Kiebel S.An introduction to random field theory. In : Frackowiak RSJ, Friston KJ, Frith CD, Dolan RJ, Price CJ, Zeki S, Ashburner J and Penny WD (eds.). Human brain function. Amsterdam : Elsevier Academic Press, 2004 : 867 – 879.

[24] Tortora GJ, Grabowski SR. Principles of anatomy and physiology (10th ed.). New Jersey : John Wiley & Sons Inc., 2002.

[25] Kim DS, Ronen I, Olman C, Kim SG *et al*. Spatial relationship between neuronal activity and BOLD functional MRI. NeuroImage 2004; 21 : 876 – 885.

[26] Logothetis NK, Pfeuffer J. On the nature of the BOLD fMRI contrast mechanism. Mag Res Ima 2004; 22 : 1517 – 1531.

[27] Thulborn KR, Wateron JC, Matthews PM *et al*. Oxygenation dependence of the transverse relaxation time of water protons in whole blood at high field. Biochem Biophys Acta. 1982; 714 : 265 – 270.

[28] Howseman AM, Bowtell RW. Functional magnetic resonance imaging : imaging techniques and contrast mechanisms. Phil Trans R Soc Lond 1999; B354 : 1179 – 1194.

[29] Pauling L, Coryell CD. The magnetic properies and structure of hemoglobin, oxyhemoglobin and carbonmonoxyhemoglobin. Proc Natl Acad Sci 1936; 22 : 210 – 216.

[30] Nair DG. About being BOLD. Brain Research Reviews 2005; 50 : 229 – 243.